Binary and Ternary Doping of Nitrogen, Boron, and Phosphorus into Carbon for Enhancing Electrochemical Oxygen Reduction Activity

Chang Hyuck Choi, Sung Hyeon Park, and Seong Ihl Woo*

Department of Chemical and Biomolecular Engineering, Korea Advanced Institute of Science and Technology, Daejeon, 305-701, Republic of Korea

ABSTRACT

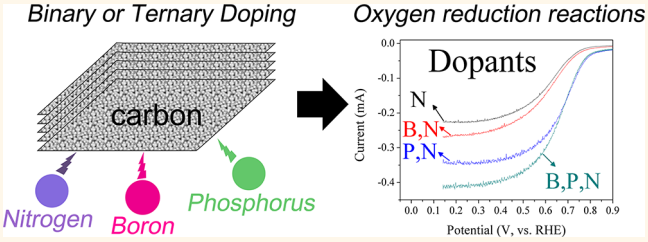

N-doped carbon, a promising alternative to Pt catalyst for oxygen reduction reactions (ORRs) in acidic media, is modified in order to increase its catalytic activity through the additional doping of B and P at the carbon growth step. This additional doping alters the electrical, physical, and morphological properties of the carbon. The B-doping reinforces the sp^2-structure of graphite and increases the portion of pyridinic-N sites in the carbon lattice, whereas P-doping enhances the charge delocalization of the carbon atoms and produces carbon structures with many edge sites. These electrical and physical alternations of the N-doped carbon are more favorable for the reduction of the oxygen on the carbon surface. Compared with N-doped carbon, B,N-doped or P,N-doped carbon shows 1.2 or 2.1 times higher ORR activity at 0.6 V (*vs* RHE) in acidic media. The most active catalyst in the reaction is the ternary-doped carbon (B,P,N-doped carbon), which records −6.0 mA/mg of mass activity at 0.6 V (*vs* RHE), and it is 2.3 times higher than that of the N-doped carbon. These results imply that the binary or ternary doping of B and P with N into carbon induces remarkable performance enhancements, and the charge delocalization of the carbon atoms or number of edge sites of the carbon is a significant factor in deciding the oxygen reduction activity in carbon-based catalysts.

KEYWORDS: oxygen reduction reactions · nitrogen · boron · phosphorus · carbon · doping

As a new non-noble metal catalyst for oxygen reduction reactions (ORRs) in acidic media, N-doped carbon has attracted much attention due to its low price and high stability in acidic media compared with commercial noble metal catalysts (*e.g.*, Pt or Pd).[1−3] However, alternatives of noble metal catalysts for N-doped carbon in commercial markets have limitations due to the relatively low ORR activity in acidic media. In order to optimize carbon-based materials as ORR catalysts, it is important to understand the nature of the reaction mechanisms and the effects of the physical characteristics of the carbon catalysts on the ORRs. Many researchers have proposed various ORR mechanisms and key factors that can determine the ORR activity of carbon-based catalysts.[4−6]

An important characteristic related to the ORR activity of carbon-based catalysts is the charge delocalization of the carbon atoms. Gong *et al.* suggested an ORR mechanism using the phenomena of the charge delocalization in carbon atoms that was induced by nitrogen doping into the carbon.[4] An oxygen molecule was adsorbed on the two carbon atoms, adjacent to the doped nitrogen, through the side-on adsorption mode. The two positively charged carbon atoms efficiently weakened the O−O bonding and then reduced the oxygen to water. Zhang *et al.* also proposed similar results in acidic media, where the doped nitrogen induced asymmetric atomic charge density and resulted in ORR activity.[7] Moreover, it was reported that there are various characteristics that can also affect the catalytic activity of carbon-based materials such as the carbon edge sites, N-doping amount, type of N-doping, surface area of micropores, and degree of sp^2-bonding in the carbon network.[6,8−10]

Various state-of-the-art techniques have been developed recently in order to modify the carbon-based catalysts, decorating them with desired features for the ORRs; these techniques involve at least a two-step process that includes secondary pyrolysis of a prepared carbon-based catalyst with an N-containing precursor,[1,11] use of sacrificial supports such as silica in the pyrolysis

* Address correspondence to siwoo@kaist.ac.kr.

Received for review May 14, 2012 and accepted July 7, 2012.

Published online July 07, 2012
10.1021/nn3021234

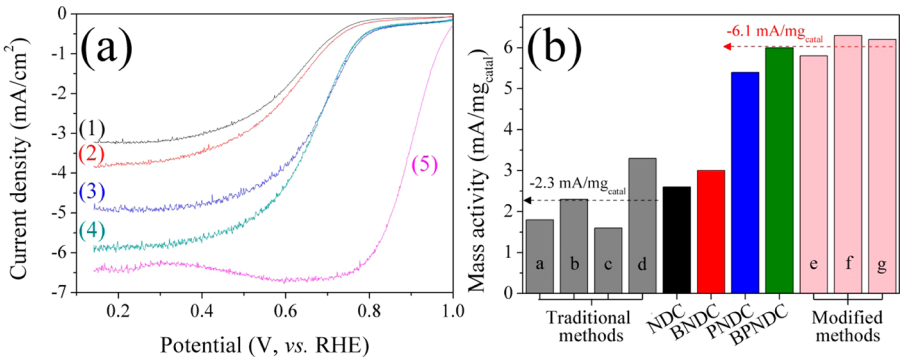

Figure 1. (a) ORR results in 1 M $HClO_4$ for the prepared catalysts: (1) NDC, (2) BNDC, (3) PNDC, (4) BPNDC, and (5) Pt/C (40 wt %). (b) Calculated mass activities at 0.6 V (*vs* RHE) for the prepared catalysts and N-doped catalysts reported by other research groups: N-doped carbon prepared by traditional methods (a to d, pyrolysis of C−N containing precursor) and by modified methods (e to g, secondary pyrolysis or use of sacrificial supports). Arrows indicate average ORR mass activities of N-doped carbons obtained from the traditional methods (a to d) and the modified methods (e to g), respectively.

step,[11,12] and modification of the carbon pore using a pore filler with small amounts of transition metals followed by a second pyrolysis.[13]

Herein, a new approach to advance the nature of carbon-based materials as ORR catalysts is presented. In contrast with previous methods, including the secondary pyrolysis step or modification of carbon pores, a different strategy to modify the carbon-based catalyst is introduced: the binary or ternary doping of heteroatoms (*e.g.*, B, P, and N) into the carbon structure without further pyrolysis. In particular, this is the first report of ternary-doped carbon being adapted as an ORR catalyst. Recently, B- and P-doped carbon without N-doping and B,N-doped carbon were proposed as ORR catalysts in alkaline media;[14−16] however, activities of the materials in acidic media were not studied, and carbon modified by binary and ternary doping of heteroatoms has not yet been applied to catalysts for ORRs extensively.

In essence, N-doped carbon (NDC) was synthesized *via* pyrolysis of a homogeneous mixture composed of dicyandiamide , $CoCl_2$, and $FeCl_2$. The additional doping of B and/or P into N-doped carbon was performed through the addition of boric acid or phosphoric acid in the homogeneous mixture before the pyrolysis step. As a result, binary-doped carbons (B,N-doped carbon (BNDC) and P,N-doped carbon (PNDC)) and a ternary-doped carbon (B,P,N-doped carbon (BPNDC)) were prepared. The modification of carbon through additional doping and its effects on the electrochemical properties are discussed comprehensively in this article.

RESULTS AND DISCUSSION

Figure 1a shows the catalytic activities for the prepared catalysts in aerated 1 M $HClO_4$. Regardless of the additional dopant types, all NDC-based catalysts demonstrated similar onset potentials toward ORRs near 0.83 V (*vs* RHE). However, the currents from the ORRs showed various values according to the type of dopants used in additional doping. The performance of the ORRs was improved through the additional doping of B and/or P. The ORR activities of the prepared catalysts were in the order BPNDC > PNDC > BNDC > NDC, with the catalyst showing the highest activity being BPNDC. The ORR activity of BPNDC was compared with that of Pt/C in Figure 1a. For numerical examinations, the mass activities (mA/mg$_{catal}$) of the catalysts were calculated at 0.6 V (*vs* RHE) (Figure 1b). The prepared catalysts recorded −2.6, −3.0, −5.4, and −6.0 mA/mg$_{catal}$ of mass activities for NDC, BNDC, PNDC, and BPNDC, respectively. After the additional B-doping (NDC to BNDC, and PNDC to BPNDC), the ORR activities of the catalysts increased by 15% and 11%, respectively. For the additional P-doping (NDC to PNDC, and BNDC to BPNDC), the activities increased 108% and 100%, respectively. Comparing the modifications of the additional B- or P-doping, it was found that the P-doping has more than 7-fold higher effects on the ORR mass activity of the NDC-based catalyst than B-doping.

BPNDC, which demonstrated the highest activity among the prepared catalysts (−6 mA/mg$_{catal}$) with good stability (Figure 2a and Figure S1), had an enhanced ORR activity compared with the traditional N-doped carbon catalysts reported by other research groups (*ca.* −2.3 mA/mg$_{catal}$, a to d in Figure 1b).[17−19] This activity is comparable to that of carbon-based catalysts prepared by modified methods (*ca.* −6.1 mA/mg$_{catal}$, e to g in Figure 1b);[1,11,12,20] therefore, it can be concluded that additional doping of other heteroatoms in N-doped carbon is an effective method to enhance ORR activity of carbon-based catalysts as well as the secondary pyrolysis and the use of sacrificial supports.

Not only the ORR activity but also the ORR pathway were positively modified to a four-electron pathway when P was additionally doped onto the NDC-based catalysts (Figure 2b). In ORRs, the oxygen is reduced to two different products: H_2O (four-electron pathway)

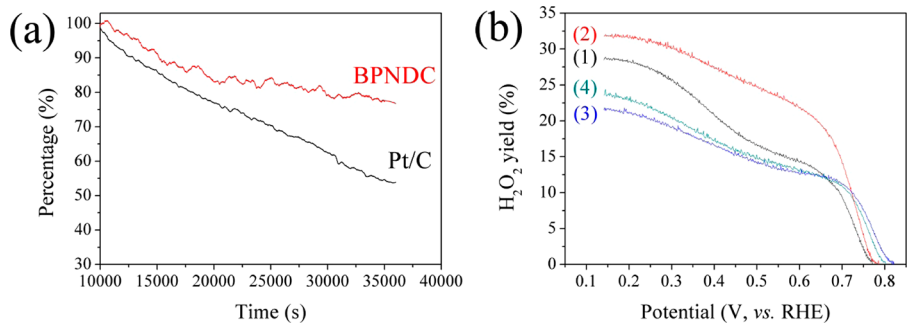

Figure 2. (a) Current−time chronoamperometric response (0.6 V, *vs* RHE) of BPNDC and Pt/C for 10 h in 1 M $HClO_4$ with continuous oxygen bubbling and (b) H_2O_2 production yields during the ORRs, calculated from the currents at the Pt-ring disk electrode (uncertainty = ±2.5%); (1) NDC, (2) BNDC, (3) PNDC, and (4) BPNDC.

and H_2O_2 (two-electron pathway). The two-electron pathway decreases the cell potential in PEMFCs and accelerates the degradation of membrane and catalysts by reacting with H_2O_2. Therefore, the four--electron pathway is desired in ORRs, but it has been reported that carbon-based catalysts generally show high H_2O_2 production yields compared with those of Pt catalysts. The H_2O_2 yields increased exponentially in the kinetic region (from 0.8 to 0.6 V, *vs* RHE), and they exhibited a gradual increase in the diffusion region (<0.6 V, *vs* RHE). The NDC recorded a 14.2% of H_2O_2 yield at 0.6 V (vs. RHE), but this was altered by the additional doping of B and P. When B was additionally doped (BNDC), 21.8% of H_2O_2 was generated at 0.6 V (*vs* RHE). However, when P was additionally doped, the H_2O_2 yield was reduced to 12.6%. The BPNDC exhibited a 13.1% H_2O_2 yield, which is slightly higher than the value of PNDC. Therefore, it can be concluded that the additional P-doping in the N-doped carbon, contrary to B-doping, induces an increase toward the four-electron pathway, and this is desired for a carbon catalyst in ORRs.

The physical properties of the prepared catalysts were characterized in order to understand how the additional B- and/or P-doping increased the ORR activity of the NDC-based carbon. The bulk compositions of the prepared catalysts were examined *via* EA and ICP analysis, which revealed the presence of B and/or P in the N-doped carbon (Table S1). The XPS analysis also supports that B and/or P is doped into the N-doped carbon at the surface of the catalysts (Table S2). The doping concentrations at the surface were higher than that at the bulk of the catalysts, and this indicates that the doping at the carbon surface is more desired than at the bulk. At the surface, the NDC discloses 3.6% N-doping, and the N-doping concentration increases to 6.8%, 5.5%, and 9.1% with the additional doping of B, P, and both B and P, respectively. This result demonstrates that additional doping of B and/or P, especially B-doping, increases the amount of nitrogen doped in the carbon. The BNDC and BPNDC show 3.4% and 4.3% B-doping concentrations, respectively. However, the P-doping concentrations had low values, under 0.6%, in both PNDC and BPNDC.

Figure 3a shows the XPS-N_{1s} results for the prepared catalysts, and it is deconvoluted using three different binding energies: pyridinic-N (N1), graphitic- or pyrrolic-N (N2), or pyridinic oxide (N3).[21] In Figure 3a, the NDC and PNDC exhibited similar shapes in the XPS-N_{1s} peaks. However, the BNDC showed an intense N1 peak compared with that of the NDC, as did BPNDC compared with PNDC. Approximately 10−15% of the pyridinic-N sites at the carbon surface were increased after the additional B-doping (Table S3). B is presented in the form of BC_3 (B1), partially oxidized B (B2, *e.g.*, BN_3, BCO_2, and BC_2O), and boron oxide (B3), as shown in Figure 3b.[22−24] The results indicate that B1 and B2 are the dominant phases of the doped B in carbon (Table S3). For P, it is doped in the form of Me_xP (P1; Me = Co or Fe, x = 1, 2), P−O (P2), and P−C (P3),[25−27] with P−O being the dominant phase (Table S3).

If all the doped N atoms participate in creating active sites for the ORR, the number of active sites, calculated using the BET area (Figure S2a) and N-doping concentration, is on the order of PNDC > BPNDC > NDC > BNDC (see SI). However, the ORR activity of the catalysts is in the order BPNDC > PNDC > BNDC > NDC. These orders do not correspond well with each other; therefore, it can be concluded that increasing N-doping concentration, through additional B- and/or P-doping, is not a crucial factor in determining the ORR activity. This conclusion is also supported by another research group's report that even N atoms induce active sites in the ORRs, but the number of N atoms able to participate in the reaction is well in excess regardless of the amount of doped N.[9] Otherwise, Ozaki *et al.* reported that the additional B-doping in the N-doped carbon increased the ORR activity and argued that this increase resulted from the generation of a new active site (B−N−C) that had 189.5 eV of binding energy in the XPS-B_{1s}.[23] However, neither BNDC nor BPNDC exhibited peaks at this position, and this indicates that the B−N−C active site is not formed in the catalysts. Moreover, residual metals that are used for carbonization of dicyandiamide cannot participate in the ORR. It was reported that metals bonded with nitrogen (MeN_x, x = 2−4) act as ORR

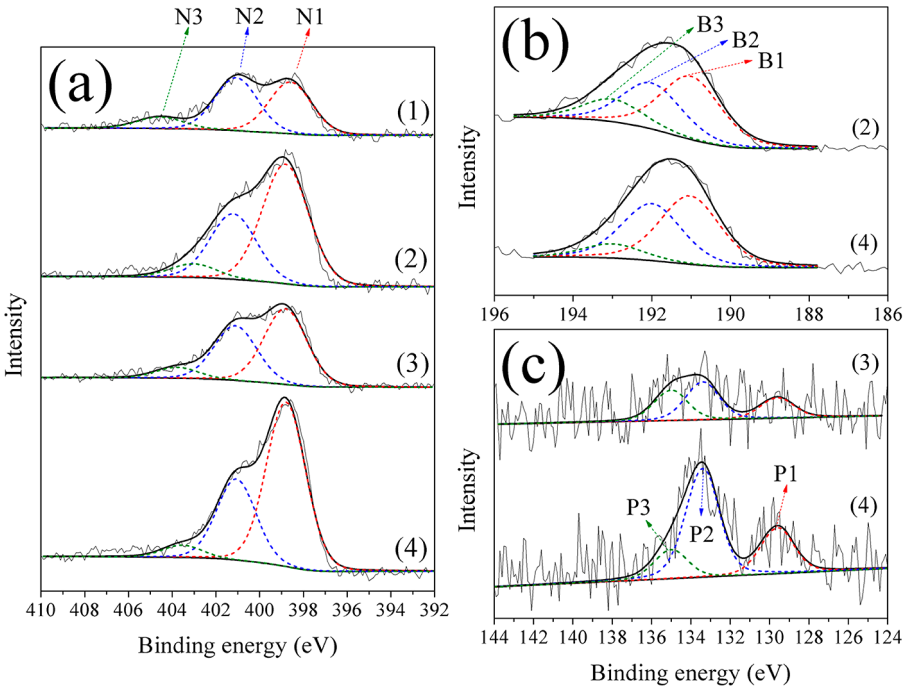

Figure 3. Analysis of the doping types for (a) N, (b) B, and (c) P in the prepared catalysts: (1) NDC, (2) BNDC, (3) PNDC, and (4) BPNDC. The XPS results are deconvoluted with (a) N1 (pyridinic-N), N2 (graphitic- or pyrrolic-N), and N3 (pyridinic oxide) for XPS-N_{1s}, (b) B1 (BC_3), B2 (partially oxidized B), and B3 (boron oxide) for XPS-B_{1s}, and (c) P1 (metal phosphide), P2 (P−O), and P3 (P−C) for XPS-P_{2p}.

active sites;[28] however, the metals including metal−nitrogen complex and metal phosphide, which were exposed at the surface of the catalysts, were dissolved by iterative acid treatment in this experiment. Therefore, there is no metal exposed at the surface of the catalysts. The CV experiments support the results (Figure S3a); the CVs of the prepared catalysts are a result of capacitance of carbon without obvious oxidation and reduction peaks of metals; thus, it can be known that there is no metal or its complex with N or P exposed at the surface of the catalysts.

It is suggested that enhanced ORR activity of the carbon-based catalysts through additional doping of B and/or P might be due to asymmetric spin density of carbon atoms induced by addional B- and/or P-doping.[7] It was reported that N-doping into carbon induces positively charged carbon atoms due to higher electronegativity of N (3.04) than that of C (2.55) and results in an increase of ORR activity.[4] Moreover, it was revealed that only B-doping or P-doping into carbon caused a break of electroneutralities due to the lower electronegativity of B (2.04) or P (2.19) than that of C and demonstrated good ORR activities in alkaline media by producing ORR active sites, positively charged dopant atoms (*e.g.*, B and P);[14,15] however, it is a diametrical mechanism compared to that of N-doping in carbon. Therefore, asymmetric charge density can be offset because of opposite properties between N-doping (inducing positive charge in carbon atoms) and B- or P-doping (inducing negative charge in carbon atoms), when B and/or P are additionally doped into N-doped carbon. Otherwise, it was proposed that asymmetric spin density of carbon atoms, which is introduced by other heteroatoms, was more important in determining ORR activities for the carbon-based materials.[7] Therefore, it could be one of the reasons for improved ORR activity that additional B- and/or P-doping enhances asymmetric spin density of carbon atoms in N-doped carbon.

As well as spin density in carbon, additional doping of B and/or P in N-doped carbon alters physical properties, and it can affect ORR activity of the carbon. The additional B-doping in the NDC-based catalysts improves 11−15% of the ORR activity. This improvement results from the increased pyridinic-N-doping induced by the additional B-doping. It has been reported previously that pyridinic-N sites have the highest ORR activity among various types of doped N.[17,29] As shown in Figure 3a and Table S3, the additional B-doping induces an increase of the pyridinic-N type at the surface of the NDC-based catalysts. Another positive effect of the additional B-doping on NDC-based catalysts is the reinforcement of the graphitic structure. Figure 4a shows the XRD results of the prepared catalyst. All catalysts exhibited graphite and some metal residue peaks in the XRD patterns. The residual metal presented after iterative acid treatment was due to carbon layers covering the metal and blocking the diffusion of protons.[30] A comparison of the intensity of the graphite (002) peak for NDC−BNDC or PNDC−BPNDC shows an increase in the peak after B-doping. This indicates that the crystalline structure of the graphite is

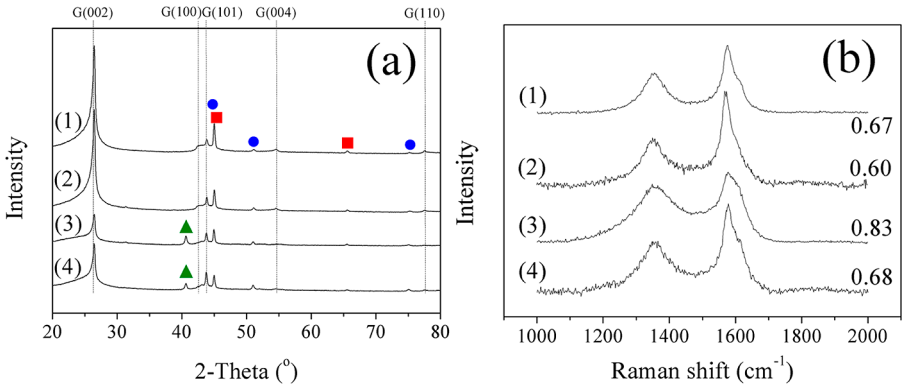

Figure 4. Characterizations for the degree of sp^2-carbon structure in the prepared catalysts: (1) NDC, (2) BNDC, (3) PNDC, and (4) BPNDC. (a) XRD results of the prepared catalysts. G(xxx) indicates a graphite peak of the (xxx) plane, while the circles, squares, and triangles denote metallic Co, Fe, and Co_2P, respectively. (b) Raman spectra results of the prepared catalysts, and the calculated I_D/I_G values are also presented.

reinforced through B-doping. The Raman spectroscopy results also support the XRD results (Figure 4b). In the Raman spectroscopy of all sp^2-carbons, two conspicuous peaks emerged near 1580 cm^{-1} of the G band and 1352 cm^{-1} of the D band. The ratio of the D and G band intensities (I_D/I_G) is generally used as a measure of carbon disorder, and a high I_D/I_G value indicates high defects in the carbon structure.[31] The I_D/I_G values for the prepared catalysts are noted in Figure 4b. The I_D/I_G value of NDC (0.67) was higher than that of BNDC (0.60), and the I_D/I_G value of PNDC (0.83) was also higher than that of BPNDC (0.68). This indicates that the B-doping reduces defect sites in the NDC-based carbon and reinforces the degree of sp^2-carbon. ORR involves the transfer of electrons to an active site; therefore, the increased electron conductivity through enhancing the degree of sp^2-carbon improves the ORR activity of the carbon-based catalysts.[10,32−34]

Moreover, not only the additional B-doping but also the P-doping improve the ORR activity of the NDC-based catalysts by 100−108%, which is significantly higher than that of the B-doping. Figure 5a shows the XPS-C_{1s} peaks of the prepared catalysts. The XPS-C_{1s} peaks of NDC and BNDC show similar results, indicating the binding energy of the C−C bond at 284.65 eV. The bare graphite shows the peak of the C−C bond at 284.5 eV,[35] but that of NDC and BNDC are up-shifted by 0.15 eV. This means that electrons from the C atoms were transferred to the doped N atoms, which has already been reported by many other research groups.[36−38] Gong *et al.* argued that this charge delocalization in the N-doped carbon provided oxygen adsorption sites in the form of side-on adsorption, and it was an active site for the ORRs by weakening the O−O bond intensity.[4] After the additional P-doping, PNDC and BPNDC exhibited peaks of the C−C bond at 284.73 eV, which is of 0.23 eV higher binding energy than that of bare graphite, and this indicates that more electrons from C are transferred. That is, the charge delocalization at the carbon atoms is enhanced by the additional P-doping. Therefore, the intensity of the O−O bonding in an oxygen molecule, which is adsorbed on the carbon atoms of PNDC or BPNDC, can be further weakened compared with that of NDC and BNDC, which indicates an increase of catalytic activity. As mentioned before, theoretical calculations showed that P-doping in carbon induces negatively delocalized C atoms adjacent to P atoms, because of the lower electronegativity of P than that of C; this results in a negative charge density in the carbon atoms.[14] However, contrary to the previous calculations, the XPS results show enhanced positive charge density after P-doping. This is because of different doping phases in the previous calculations and PNDC-BPNDC samples; the calculations were based on P−C direct bonding, but a dominant P-doping type in PNDC and BPNDC is the P−O phase (42.8% and 59.2% in PNDC and BPNDC, respectively), as shown in Figure 3c. This means an oxygen bridge is formed between P and C (P−O−C bonding), and the oxygen atoms having higher electronegativity (3.44) can enhance electron poverty in the carbon atoms.

Furthermore, the additional P-doping alters the morphology of the NDC-based catalysts. Figure 5b shows the TEM images of the prepared catalysts. NDC and BNDC have a horn-like structure, but PNDC and BPNDC show a bamboo-like CNT structure. As shown in Figure 5b, the magnified image of the BNDC (similar to NDC) indicates that several carbon layers are stacked on each other. However, PNDC (similar to BPNDC) shows an uneven surface morphology and many open edge sites that are split and wrinkled. The covalent radius of B is 84 ± 3 pm, and it forms an sp^2-orbital as its constructing structure. These physical characteristics are very similar to those of carbon, which has a 73 pm covalent radius and forms a sp^2-orbital in graphite. On the other hand, P exhibits a covalent radius of 107 ± 3 pm and favors the sp^3-orbital configuration in molecules. Therefore, P-doping in the carbon lattice generates a high distortion of carbon structures and finally allows many open edge sites and a wrinkled morphology of the carbon.

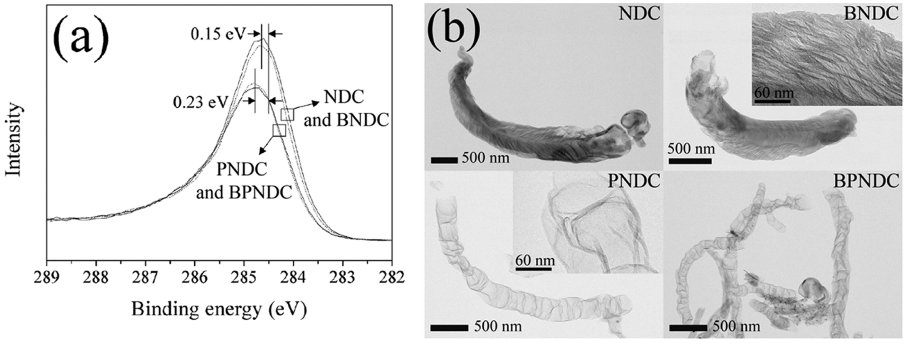

Figure 5. Effects of the additional P-doping in the prepared catalysts: (a) XPS-C_{1s} spectroscopy and (b) TEM images of the prepared catalysts. Magnified images of BNDC and PNDC are inset in each figure.

Recently, many experimental and theoretical studies have supported that the ORR is more favorable at the carbon edge sites than at the middle of carbon surface.[5,6,21,29] In this manner, the production of many edge sites resulting from the additional P-doping is also a cause of the improved ORR activity for PNDC and BPNDC.

CONCLUSIONS

In conclusion, the ability of N-doped carbon as a catalyst for ORR was developed through the additional doping of B and/or P. It is suggested that additional doping of B and/or P enhances asymmetry atomic spin density. Moreover, the experimental results demonstrated that the additional doping of B and/or P modifies the carbon characteristics and improves the ORR activity of the NDC-based catalysts. The B-doping increases the portion of pyridinic-N sites among various N-doping types and magnifies the degree of the sp^2-carbon structures. However, the P-doping enhances the charge delocalization of the carbon atoms and constructs morphology with many open edge sites that are split and wrinkled. The ORR activities of the NDC-based catalysts were increased by 11−15% due to the additional B-doping, but there was an increase of 100−108% in the case of additional P-doping. Therefore, it can be concluded that the charge delocalization of the carbon atoms or the number of open edge sites is a significant factor in determining the ORR activity of N-doped carbon rather than doped N types or degree of sp^2-carbon. The catalyst demonstrating the best ORR activity was BPNDC, where both B and P were additionally doped in the NDC, and it demonstrated a −6.0 mA/mg mass activity at 0.6 V (*vs* RHE), which is 2.3 times higher than that of NDC.

METHODS

Catalyst Preparation. N-doped carbon was prepared *via* pyrolysis of a homogeneous mixture consisting of dicyandiamide (DCDA) and metal chlorides. Briefly, DCDA (5 g, Aldrich), $FeCl_2{-}4H_2O$ (3.8 mmol, Yakumi Pure Chemical Co. Ltd.), and $CoCl_2{-}6H_2O$ (9.5 mmol, Aldrich) were dissolved in 100 mL of DI water *via* stirring for 30 min. The solvent was removed using an evaporator (Buchi R-200) operated at 80 °C and 300 mbar. The prepared gel-like mixture was dried in an oven at 80 °C overnight. After grinding, the powder was loaded on quartz boats, and then it was placed in the middle of a quartz tube reactor. Pyrolysis of the powder was performed at 900 °C for 3 h under 50 cm^3/min of Ar atmosphere. The pyrolyzed composite was stirred in 300 mL of aqua regia (Dae Jung) in order to dissolve the Fe and Co particles in the carbon. Finally, the catalysts were filtered, washed with DI water, and then dried in an oven. The B,N-doped carbon, P,N-doped carbon, and B,P,N-doped carbon were synthesized using similar preparation methods to those of NDC, but with the addition of B and P precursors in the precursor mixture. Boric acid (4.0 mmol, Aldrich) and/or phosphoric acid (2.6 mmol, Aldrich) were added in a round flask, which already contained DCDA, metal chlorides, and water. After that, the evaporation, drying, pyrolysis, and acid treatment steps were followed.

Electrochemical Characterizations. The electrochemical properties were examined using a three-electrode beaker cell equipped with a Pt wire counter electrode (ALS Co., 002233), an Ag/AgCl reference electrode (ALS Co., 012167), and a rotating ring disk electrode (ALS Co., 011162), using an electrochemical analyzer (CH Instruments Inc., CHI700D) and a rotator (ALS Co., RRDE-3A). The working electrodes were prepared *via* the thin film electrode method. The catalysts (10 mg) were dispersed in an ink solution (1 mL; DI water (15), 5 wt % Nafion in water (4), isopropyl alcohol (1); the number in parentheses indicates the volumetric ratio) followed by sonication, and then catalyst inks (5 μL) were dropped onto glassy carbon in a rotating ring disk electrode. The catalyst inks were dried at room temperature. Twenty cycles of cyclic voltammetry (CV) experiments were conducted in deaerated 1 M $HClO_4$ electrolyte for activation of the catalysts with a 15 mV/s scan rate from −0.220 to 0.578 V (*vs* Ag/AgCl). The data from the last cycle were selected for characterization. The ORR experiments were conducted in O_2-saturated 1 M $HClO_4$ electrolyte with a 5 mV/s scan rate and 2000 rpm rotating velocity from 0.82 to −0.08 V (*vs* Ag/AgCl). For comparison of the ORR activity, commercially obtained Pt/C (40 wt %, E-tek) was also examined in the same conditions. Stability was examined by current−time chronoamperometry at 0.38 V (*vs* Ag/AgCl) for 10 h in 1 M $HClO_4$ with continuous oxygen bubbling and by obtaining ORR performance after 200 cycles of CV in 1 M $HClO_4$ with a 30 mV/s scan rate from 0.9 to 1.3 V (*vs* Ag/AgCl). The H_2O_2 formation yield was derived from the current at the Pt ring disk electrode. A constant potential (1.0 V, *vs* Ag/AgCl) was applied on the Pt ring disk electrode during the ORR experiment. The following equation was used to calculate the H_2O_2 formation yield:

$$H_2O_2(\%) = 200 \times \frac{I_R/N}{I_R/N + I_D}$$

where I_R and I_D are the ring and disk currents, respectively, and N is the collection efficiency (0.37). All potentials shown in this

paper were converted to reversible hydrogen electrode (RHE) scale.

Physical Characterization. The physical properties of the prepared catalysts were examined *via* element analysis (EA), inductively coupled plasma (ICP), X-ray photoelectron spectroscopy (XPS), Brunauer–Emmett–Teller (BET) surface area analysis, X-ray diffraction (XRD), Raman spectroscopy, transmission electron microscopy (TEM), and thermogravimetry (TGA). The experimental details are as follows. An EA was performed in order to obtain the bulk compositions of the catalysts using a FlashEA 1112. The amounts of B and P in the carbons were obtained *via* ICP analysis (POLY SCAN 61 E). The XPS analysis was performed using a Sigma Probe (Thermo VG Scientific) equipped with a microfocused monochromator X-ray source. The doping concentration of the dopants in the carbon was expressed using the atomic ratio of the dopant atoms to the carbon atoms measured *via* EA–ICP or XPS. A BET surface area analysis was performed using a Micrometrics ASAP 2010 apparatus at 77 K. Before measurement, all samples were degassed and dehydrated at 200 °C for 2 h. The XRD patterns were acquired using a D/MAX-2500 (Rigaku) operated at 40 kV and 100 mA. The step-scan patterns were collected in the 20–80° (2-theta ranges) range with 0.01° step size and 1 deg/min scan speed. The data from Raman spectroscopy were obtained using a LabRAM HR UV/vis/NIR with a 514 nm Ar ion CW laser source. The TEM images were taken with a JEM2100-F (Jeol Ltd.) operated at 200 kV. The TGA results were obtained from LABSYS evo (Setaram) under an air atmosphere.

Conflict of Interest: The authors declare no competing financial interest.

Supporting Information Available: Bulk and surface compositions, doping types and fractions, BET surface areas and average pore sizes, stability tests, TGA results, CVs results, and calculated specific activities. This material is available free of charge *via* the Internet at http://pubs.acs.org.

Acknowledgment. This work was supported by the National Research Foundation of Korea (NRF) grant funded by the Korea government (MEST) (No. 2011-0029812).

REFERENCES AND NOTES

1. Wu, G.; More, K. L.; Johnston, C. M.; Zelenay, P. High-Performance Electrocatalysts for Oxygen Reduction Derived from Polyaniline, Iron, and Cobalt. *Science* **2011**, *332*, 443–447.
2. Xiong, W.; Du, F.; Liu, Y.; Perez, A.; Supp, M.; Ramakrishnan, T. S.; Dai, L. M.; Jiang, L. 3-D Carbon Nanotube Structures Used as High Performance Catalyst for Oxygen Reduction Reaction. *J. Am. Chem. Soc.* **2010**, *132*, 15839–15841.
3. Sidik, R. A.; Anderson, A. B.; Subramanian, N. P.; Kumaraguru, S. P.; Popov, B. N. O2 Reduction on Graphite and Nitrogen-Doped Graphite: Experiment and Theory. *J. Phys. Chem. B* **2006**, *110*, 1787–1793.
4. Gong, K. P.; Du, F.; Xia, Z. H.; Durstock, M.; Dai, L. M. Nitrogen-Doped Carbon Nanotube Arrays with High Electrocatalytic Activity for Oxygen Reduction. *Science* **2009**, *323*, 760–764.
5. Ikeda, T.; Boero, M.; Huang, S. F.; Terakura, K.; Oshima, M.; Ozaki, J. Carbon Alloy Catalysts: Active Sites for Oxygen Reduction Reaction. *J. Phys. Chem. C* **2008**, *112*, 14706–14709.
6. Kim, H.; Lee, K.; Woo, S. I.; Jung, Y. On the Mechanism of Enhanced Oxygen Reduction Reaction in Nitrogen-Doped Graphene Nanoribbons. *Phys. Chem. Chem. Phys.* **2011**, *13*, 17505–17510.
7. Zhang, L. P.; Xia, Z. H. Mechanisms of Oxygen Reduction Reaction on Nitrogen-Doped Graphene for Fuel Cells. *J. Phys. Chem. C* **2011**, *115*, 11170–11176.
8. Choi, C. H.; Lee, S. Y.; Park, S. H.; Woo, S. I. Highly Active N-doped-CNTs Grafted on Fe/C Prepared by Pyrolysis of Dicyandiamide on Fe_2O_3/C for Electrochemical Oxygen Reduction Reaction. *Appl. Catal. B: Environ.* **2011**, *103*, 362–368.
9. Jaouen, F.; Herranz, J.; Lefevre, M.; Dodelet, J. P.; Kramm, U. I.; Herrmann, I.; Bogdanoff, P.; Maruyama, J.; Nagaoka, T.; Garsuch, A.; *et al.* Cross-Laboratory Experimental Study of Non-Noble-Metal Electrocatalysts for the Oxygen Reduction Reaction. *ACS Appl. Mater. Interfaces* **2009**, *1*, 1623–1639.
10. Niwa, H.; Kobayashi, M.; Horiba, K.; Harada, Y.; Oshima, M.; Terakura, K.; Ikeda, T.; Koshigoe, Y.; Ozaki, J.; Miyata, S.; *et al.* X-ray Photoemission Spectroscopy Analysis of N-Containing Carbon-Based Cathode Catalysts for Polymer Electrolyte Fuel Cells. *J. Power Sources* **2011**, *196*, 1006–1011.
11. Liu, G.; Li, X. G.; Lee, J. W.; Popov, B. N. A Review of the Development of Nitrogen-Modified Carbon-Based Catalysts for Oxygen Reduction at USC. *Catal. Sci. Technol.* **2011**, *1*, 207–217.
12. Liu, G.; Li, X. G.; Ganesan, P.; Popov, B. N. Studies of Oxygen Reduction Reaction Active Sites and Stability of Nitrogen-Modified Carbon Composite Catalysts for PEM Fuel Cells. *Electrochim. Acta* **2010**, *55*, 2853–2858.
13. Lefevre, M.; Proietti, E.; Jaouen, F.; Dodelet, J. P. Iron-Based Catalysts with Improved Oxygen Reduction Activity in Polymer Electrolyte Fuel Cells. *Science* **2009**, *324*, 71–74.
14. Liu, Z. W.; Peng, F.; Wang, H. J.; Yu, H.; Zheng, W. X.; Yang, J. A. Phosphorus-Doped Graphite Layers with High Electrocatalytic Activity for the O_2 Reduction in an Alkaline Medium. *Angew. Chem., Int. Ed.* **2011**, *50*, 3257–3261.
15. Yang, L. J.; Jiang, S. J.; Zhao, Y.; Zhu, L.; Chen, S.; Wang, X. Z.; Wu, Q.; Ma, J.; Ma, Y. W.; Hu, Z. Boron-Doped Carbon Nanotubes as Metal-Free Electrocatalysts for the Oxygen Reduction Reaction. *Angew. Chem., Int. Ed.* **2011**, *50*, 7132–7135.
16. Wang, S. Y.; Iyyamperumal, E.; Roy, A.; Xue, Y. H.; Yu, D. S.; Dai, L. M. Vertically Aligned BCN Nanotubes as Efficient Metal-Free Electrocatalysts for the Oxygen Reduction Reaction: A Synergetic Effect by Co-Doping with Boron and Nitrogen. *Angew. Chem., Int. Ed.* **2011**, *50*, 11756–11760.
17. Subramanian, N. P.; Li, X. G.; Nallathambi, V.; Kumaraguru, S. P.; Colon-Mercado, H.; Wu, G.; Lee, J. W.; Popov, B. N. Nitrogen-Modified Carbon-Based Catalysts for Oxygen Reduction Reaction in Polymer Electrolyte Membrane Fuel Cells. *J. Power Sources* **2009**, *188*, 38–44.
18. Ozaki, J.; Tanifuji, S.; Furuichi, A.; Yabutsuka, K. Enhancement of Oxygen Reduction Activity of Nanoshell Carbons by Introducing Nitrogen Atoms from Metal Phthalocyanines. *Electrochim. Acta* **2010**, *55*, 1864–1871.
19. Zhang, H. J.; Jiang, Q. Z.; Sun, L. L.; Yuan, X. X.; Shao, Z. P.; Ma, Z. F. 3D Non-Precious Metal-Based Electrocatalysts for the Oxygen Reduction Reaction in Acid Media. *Int. J. Hydrogen Energy* **2010**, *35*, 8295–8302.
20. Wu, G.; Johnston, C. M.; Mack, N. H.; Artyushkova, K.; Ferrandon, M.; Nelson, M.; Lezama-Pacheco, J. S.; Conradson, S. D.; More, K. L.; Myers, D. J.; *et al.* Synthesis-Structure-Performance Correlation for Polyaniline-Me-C Non-Precious Metal Cathode Catalysts for Oxygen Reduction in Fuel Cells. *J. Mater. Chem.* **2011**, *21*, 11392–11405.
21. Matter, P. H.; Zhang, L.; Ozkan, U. S. The Role of Nanostructure in Nitrogen-Containing Carbon Catalysts for the Oxygen Reduction Reaction. *J. Catal.* **2006**, *239*, 83–96.
22. Koh, M.; Nakajima, T. Synthesis of Well Crystallized Boron-Carbon Filament by Chemical Vapor Deposition Using a Nickel Catalyst. *Carbon* **1998**, *36*, 913–920.
23. Ozaki, J.; Kimura, N.; Anahara, T.; Oya, A. Preparation and Oxygen Reduction Activity of BN-Doped Carbons. *Carbon* **2007**, *45*, 1847–1853.
24. Jacques, S.; Guette, A.; Bourrat, X.; Langlais, F.; Guimon, C.; Labrugere, C. LPCVD and Characterization of Boron-Containing Pyrocarbon Materials. *Carbon* **1996**, *34*, 1135–1143.
25. Blanchard, P. E. R.; Grosvenor, A. P.; Cavell, R. G.; Mar, A. X-ray Photoelectron and Absorption Spectroscopy of Metal-Rich Phosphides M2P and M3P (M = Cr-Ni). *Chem. Mater.* **2008**, *20*, 7081–7088.
26. Claeyssens, F.; Fuge, G. M.; Allan, N. L.; May, P. W.; Ashfold, M. N. R. Phosphorus Carbides: Theory and Experiment. *Dalton Trans.* **2004**, 3085–3092.
27. Panwar, O. S.; Khan, M. A.; Kumar, M.; Shivaprasad, S. M.; Satyanarayana, B. S.; Dixit, P. N.; Bhattacharyya, R.

Characterization of Boron- and Phosphorous-Incorporated Tetrahedral Amorphous Carbon Films Deposited by the Filtered Cathodic Vacuum Arc Process. *Jpn. J. Appl. Phys.* **2009**, *48*, 065501.
28. Choi, J. Y.; Higgins, D.; Chen, Z. W. Highly Durable Graphene Nanosheet Supported Iron Catalyst for Oxygen Reduction Reaction in PEM Fuel Cells. *J. Electrochem. Soc.* **2012**, *159*, B87–B90.
29. Oh, H. S.; Oh, J. G.; Lee, W. H.; Kim, H. J.; Kim, H. The Influence of the Structural Properties of Carbon on the Oxygen Reduction Reaction of Nitrogen Modified Carbon Based Catalysts. *Int. J. Hydrogen Energy* **2011**, *36*, 8181–8186.
30. Choi, C. H.; Park, S. H.; Woo, S. I. N-Doped Carbon Prepared by Pyrolysis of Dicyandiamide with Various MeCl2·xH2O (Me = Co, Fe, and Ni) Composites: Effect of Type and Amount of Metal Seed on Oxygen Reduction Reactions. *Appl. Catal. B: Environ.* **2012**, *119*−*120*, 123–131.
31. Ghosh, K.; Kumar, M.; Maruyama, T.; Ando, Y. Micro-Structural, Electron-Spectroscopic and Field-Emission Studies of Carbon Nitride Nanotubes Grown from Cage-Like and Linear Carbon Sources. *Carbon* **2009**, *47*, 1565–1575.
32. Myung, H. S.; Park, Y. S.; Hong, B.; Han, J. G.; Kim, Y. H.; Lee, J. Y.; Shaginyan, L. R. Effect of the Target Power Density on the Synthesis and Physical Properties of Sputtered nc-C Films. *Thin Solid Films* **2006**, *494*, 123–127.
33. Onoprienko, A. A.; Yanchuk, I. B. Effects of Deposition Conditions on Carbon-Film Resistivity and Microstructure. *Powder Metall. Met. Ceram.* **2005**, *44*, 499–504.
34. Ismagilov, Z. R.; Shalagina, A. E.; Podyacheva, O. Y.; Ischenko, A. V.; Kibis, L. S.; Boronin, A. I.; Chesalov, Y. A.; Kochubey, D. I.; Romanenko, A. I.; Anikeeva, O. B.; *et al.* Structure and Electrical Conductivity of Nitrogen-Doped Carbon Nanofibers. *Carbon* **2009**, *47*, 1922–1929.
35. Nanse, G.; Papirer, E.; Fioux, P.; Moguet, F.; Tressaud, A. Fluorination of Carbon Blacks: An X-ray Photoelectron Spectroscopy Study 0.1. A Literature Review of XPS Studies of Fluorinated Carbons. XPS Investigation of Some Reference Compounds. *Carbon* **1997**, *35*, 175–194.
36. Maldonado, S.; Morin, S.; Stevenson, K. J. Structure, Composition, and Chemical Reactivity of Carbon Nanotubes by Selective Nitrogen Doping. *Carbon* **2006**, *44*, 1429–1437.
37. Lim, S. H.; Elim, H. I.; Gao, X. Y.; Wee, A. T. S.; Ji, W.; Lee, J. Y.; Lin, J. Electronic and Optical Properties of Nitrogen-Doped Multiwalled Carbon Nanotubes. *Phys. Rev. B* **2006**, *73*, 1–6.
38. Liu, G.; Li, X. G.; Ganesan, P.; Popov, B. N. Development of Non-Precious Metal Oxygen-Reduction Catalysts for PEM Fuel Cells Based on N-Doped Ordered Porous Carbon. *Appl. Catal. B: Environ.* **2009**, *93*, 156–165.